

## FEATURE ARTICLE

### Optical Second Harmonic Generation Studies of Azobenzene Surfactant Adsorption and Photochemistry at the Water/1,2-Dichloroethane Interface

Roberta R. Naujok, Hillary J. Paul, and Robert M. Corn\*

Department of Chemistry, University of Wisconsin—Madison, 1101 University Avenue,  
Madison, Wisconsin 53706

Received: February 23, 1996<sup>⊗</sup>

The surface-sensitive spectroscopic technique of optical second harmonic generation (SHG) is employed to study the adsorption and photochemistry of surfactant molecules at the water/1,2-dichloroethane (DCE) interface. Resonant SHG measurements at 730 nm are used to monitor the adsorption of the azobenzene surfactant 4-[[dodecyloxy]benz-4-yl]azo]benzoic acid (DBA) from DCE solution to the interface at an aqueous pH of 8 or greater. The concentration and pH dependence of the resonant SHG from the adsorbed monolayer indicates that the DBA exists in its anionic (carboxylate) form at the interface. In a series of combined photochemical/SHG experiments the *trans/cis* photoisomerization of the adsorbed DBA anions is examined. SHG measurements demonstrate that illumination of the surface with light at 365 nm converts the adsorbed *trans*-DBA molecules to the *cis* isomer. The *cis*-DBA anion is found to be unusually stable at the liquid/liquid interface, and the entire photoactive monolayer (total area 4 cm<sup>2</sup>) can be photochemically converted in approximately 450 s with an illumination spot of 0.12 cm<sup>2</sup>. This relatively short conversion time is attributed to surface-tension-induced convection effects that occur during the photochemical conversion of the monolayer. Illumination of the *cis*-DBA anions with light at 440 nm reconverts the entire surfactant monolayer back to the *trans*-DBA form in the same time frame.

#### Introduction

Many chemical processes in the fields of electrochemistry, biology, separation science, and environmental studies involve the transport or reaction of molecules at liquid/liquid interfaces. The characterization of these processes is often achieved by spectroscopically monitoring the adsorption, orientation, organization, and reactivity of submonolayer quantities of surfactant molecules adsorbed to the interface. For example, at the liquid/air interface, a variety of fluorescence experiments have been implemented in order to optically probe the structure and reactivity of amphiphiles incorporated into insoluble Langmuir

films.<sup>1–3</sup> Similar fluorescence measurements have been applied to the study of surfactants adsorbed to the liquid alkane/water interface.<sup>4–8</sup> Another liquid/liquid interface that has recently received attention is the interface between water and various polar organic liquids such as nitrobenzene or 1,2-dichloroethane (DCE).<sup>9–11</sup> These organic solvents are immiscible with water, yet are polar enough to dissolve electrolyte ions. This capability allows a potential to be applied across this interface between two immiscible electrolyte solutions (ITIES), and the transport of ions across this interface can be studied with electrochemical methods.<sup>12–20</sup> The adsorption of soluble surfactant molecules to the ITIES and other liquid/liquid interfaces has also been studied by spectroscopic methods,<sup>4–6,21–26</sup> but a major obstacle

<sup>⊗</sup> Abstract published in *Advance ACS Abstracts*, June 1, 1996.

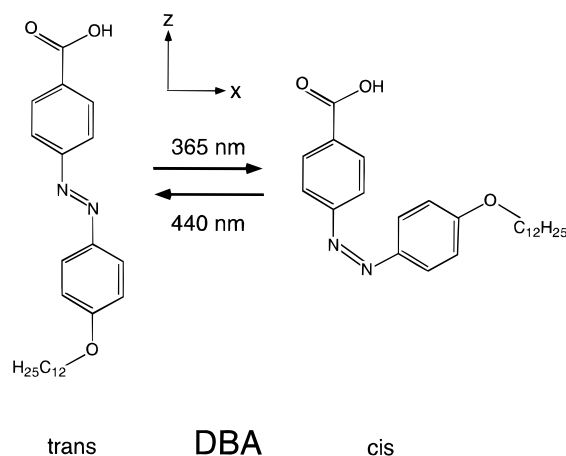


**Figure 1.** Azobenzene SHG probe molecule 4-[[dodecyloxy]benz-4-yl]azo]benzoic acid (DBA) and its reversible *trans/cis* photoisomerization reaction. Illumination of *trans*-DBA at 365 nm converts the molecule to its *cis* form. Reconversion is effected by illumination of the *cis*-DBA with 440 nm light. The *z* and *x* axes used in the molecular nonlinear polarizability calculations are illustrated.

in these measurements is the difficulty in separating the optical response of surfactants dissolved in either the organic or aqueous phase from that of the interfacial species.

Optical second harmonic generation (SHG) is one spectroscopic technique that can overcome this difficulty. SHG is the nonlinear process that converts two photons of frequency  $\omega$  to one photon of frequency  $2\omega$ . In the electric dipole approximation, this requires a noncentrosymmetric medium.<sup>27</sup> Thus, for an interface between two centrosymmetric phases, such as the liquid/liquid interface, to first order only the molecules which participate in the asymmetry of the interface will contribute to the SHG signal. This symmetry requirement usually means that only the first few molecular monolayers are responsible for the generation of second harmonic light, thus making SHG an extremely surface-selective spectroscopic method that has been applied to a wide variety of condensed phase interfaces.<sup>28–34</sup> It is this surface selectivity that makes SHG an ideal method with which to study the liquid/liquid interface, and in fact a number of SHG studies of various liquid/liquid interfaces have recently been reported.<sup>22–26,35–37</sup>

In this paper, the adsorption and photochemistry of an azobenzene derivative, 4-[[dodecyloxy]benz-4-yl]azo]benzoic acid (hereafter denoted as DBA; see Figure 1) at the water/DCE interface is examined with resonant molecular SHG measurements at 730 nm. Resonant SHG is obtained when one or more of the optical frequencies is turned into resonance with an electronic transition of an adsorbed species, and typically requires a molecule (such as DBA) which has been designed to provide a large nonlinear optical response. In addition to its nonlinear optical activity, DBA can also undergo the reversible photochemical *trans* to *cis* isomerization that is observed in azobenzenes upon exposure to UV light (Figure 1).<sup>38,39</sup> The *trans* to *cis* isomerization of an azobenzene derivative changes its dipole moment, structural geometry, and optical spectrum, and all of these properties can be exploited in different photochemical applications. For this reason, the photoisomerization of azobenzene derivatives has been intensively studied in recent years for potential use in the fields of photonics, liquid crystals, optical memory storage, artificial vision, and sensors.<sup>40–45</sup> The azobenzene isomerization process has been examined in a variety of chemical environments including incorporation into Langmuir–Blodgett films,<sup>46–51</sup> self-assembled monolayers and multilayers,<sup>52</sup> polymer films,<sup>53–56</sup> phospholipid bilayers,<sup>57,58</sup> liquid crystal films,<sup>59,60</sup> sol–gels,<sup>41,61</sup> and monolayers at the air/

water interface.<sup>62,63</sup> At the water/DCE interface, the resonant SHG measurements presented in this paper demonstrate that the adsorbed DBA molecules can be readily converted from the *trans* to *cis* form with light at 365 nm, and that the adsorbed *cis*-DBA species can be reconverted to the *trans* form upon exposure to light at 440 nm. Moreover, the *cis* form of DBA is unusually stable at the water/DCE interface, with no appreciable desorption or thermal reconversion to the *trans* form observed over several hours.

## Background

**A. Molecular Second-Order Nonlinear Polarizability Tensor,  $\beta$ .** Resonant molecular SHG measurements are used in this paper to study surfactant adsorption at the water/DCE interface. In general, there are several possible contributions to the second harmonic light generated at the liquid/liquid interface.<sup>64</sup> First, all of the oriented solvent molecules at the interface will have a weak nonlinear optical response. These nonresonant contributions to the SHG are typically small, but can be observed at liquid surfaces.<sup>36,37</sup> For example, Goh *et al.*<sup>65</sup> have used this nonresonant SHG to probe the orientation of water molecules at the air/water interface. A second possible source is “electric-field-induced SHG” due to the symmetry-breaking at a surface induced by any interfacial electrostatic field. This effect has been observed at metal, silica, and semiconductor surfaces in contact with aqueous solutions,<sup>66,67,29</sup> but is weak at the water/DCE interface.<sup>68</sup> When molecules are adsorbed to the liquid/liquid interface, a third, larger contribution to the surface SHG is often present. This “resonant SHG” is observed when the fundamental laser frequency is tuned into resonance with an electronic transition of an adsorbed molecule. Experiments that employ resonant molecular SHG usually require molecules that have been designed to provide a large nonlinear optical response, which is described by the molecular second-order nonlinear polarizability tensor,  $\beta$ .

The molecular nonlinear polarizability tensor for molecules with a conjugated  $\pi$  electron system is typically examined theoretically with a perturbation calculation that employs semiempirical Pople–Pariser–Parr (PPP) wave functions.<sup>24,69–71</sup> However, a two-state model which only considers a ground state and a single excited state is sufficient to describe the key aspects of designing a molecule with a large nonlinear optical response. In this simple two-state model, the *ijk* component of the nonlinear polarizability tensor (where *i*, *j*, and *k* are molecular Cartesian coordinates) is described by eq 1, where  $\Delta r_n$  is the

$$\beta_{ijk} = \frac{-e^3}{2\hbar^2} \left[ \frac{\Delta r_n^i r_{ng}^j r_{ng}^k}{\omega_{ng}^2 - \omega^2} + r_{ng}^i (r_{ng}^j \Delta r_n^k + \Delta r_n^j r_{ng}^k) \frac{\omega_{ng}^2 + 2\omega^2}{(\omega_{ng}^2 - 4\omega^2)(\omega_{ng}^2 - \omega^2)} \right] \quad (1)$$

difference in the permanent dipole moment between the excited state *n* and the ground state *g*,  $r_{ng}$  is the transition dipole moment between the two states,  $\omega$  is the fundamental laser frequency, and  $\omega_{ng}$  is the frequency that corresponds to the energy difference between the ground and excited states. If the change in dipole moment and the transition dipole are colinear, then only one element of  $\beta$  is dominant, usually defined as the *zzz* component. When this is the case, the polarization analysis of the SHG results is greatly simplified.<sup>72</sup>

There are three important points that can be deduced from eq 1. First,  $\beta$  has resonances at two wavelengths: the first when the fundamental laser frequency is in resonance with the electronic transition of the molecule ( $\omega_{ng}$ ) and the second when

the second harmonic frequency is in resonance with the same transition. This second resonance condition is particularly useful for surface SHG experiments, since signal enhancement can occur without significant absorption of the fundamental laser light that would lead to photobleaching of the adsorbed molecules and heating of the interface. The second is that  $\beta$  is proportional to the square of the transition dipole moment, so conjugated dye molecules with large extinction coefficients will often have a larger nonlinear polarizability. The third point is that, in addition to the transition dipole moment,  $\beta$  is directly proportional to the change in the permanent dipole moment between the two states. From the last two points, it can be seen that (i) only molecules which exhibit this change in dipole moment have a significant nonlinear polarizability and (ii) the optical transitions that are most useful for resonance enhancement are charge-transfer transitions such as those present in extended  $\pi$ -conjugation systems that have been decorated with electron donor and acceptor groups.

These concerns have resulted in a large effort to design organic nonlinear optical materials that often employ conjugated aromatic molecules with charge transfer transitions.<sup>73</sup> Since self-absorption of the second harmonic light is not a significant problem for a monolayer of material, these molecules can be used on resonance in the surface SHG experiments. One class of molecules that has been examined extensively for potential nonlinear optical applications is azobenzene and its derivatives such as the DBA probe molecule used in this paper.<sup>74–76</sup> The extended  $\pi$ -conjugation of such molecules provides for low-energy charge transfer transitions with large transition dipole moments in the blue or near-UV that can be easily accessed by near-IR and visible lasers. Also, by adding donor–acceptor substituents to the azobenzene, large excited state dipole moments can be created, making these molecules excellent choices for use in surface SHG experiments. In the case of azobenzene derivatives,  $\beta$  is sufficiently large that SHG can be observed without resonance enhancement, leading to its potential use as a nonlinear optical material.<sup>75</sup> The utilization of the resonance enhancement, however, greatly increases the SHG signal from a monolayer of these molecules, making substituted azobenzenes good probe molecules for interfacial explorations. PPP wave function calculations of the molecular nonlinear polarizability for *trans*- and *cis*-DBA are presented in the Results and Discussion.

**B. Surface Second-Order Nonlinear Susceptibility Tensor,  $\chi_s^{(2)}$ .** A monolayer of SHG-active surfactant molecules adsorbed to a liquid/liquid interface will interact with an incident laser light field in a collective fashion. This coherent surface response is described by the surface second-order nonlinear susceptibility tensor,  $\chi_s^{(2)}$ . The elements of this tensor are related to the molecular nonlinear polarizability tensor elements by eq 2, where  $N_s$  is the surface coverage of the adsorbed surfactants

$$\chi_{IJK} = N_s \sum \langle F_{IJKijk}(\xi, \theta, \alpha) \rangle \beta_{ijk} \quad (2)$$

and  $\langle F_{IJKijk} \rangle$  is the ensemble average of the product of the direction cosines between the laboratory axes  $I$ ,  $J$ , and  $K$  and the molecular axes  $i$ ,  $j$ , and  $k$ . The quantities  $F_{IJKijk}$  can be described by the Euler angles  $\xi$ ,  $\theta$ , and  $\alpha$  between the two coordinate systems. For a surface that is isotropic about the surface normal (which is usually the case for a liquid/liquid interface), there are only three unique elements of  $\chi_s^{(2)}$ , which are denoted here as  $\chi_{ZZZ}$ ,  $\chi_{ZXX}$ , and  $\chi_{XXZ}$ .<sup>72</sup>

The intensity of second harmonic light created at the interface,  $I(2\omega)$ , is related to the surface nonlinear susceptibility tensor  $\chi_s^{(2)}$  by eq 3, where  $I(\omega)$  is the incident fundamental laser light

$$I(2\omega) = \frac{32\pi^3 \omega^2 \sec^2 \theta_{2\omega}}{c^3} |\mathbf{e}(2\omega) \cdot \chi_s^{(2)} \cdot \mathbf{e}(\omega) \mathbf{e}(\omega)|^2 I(\omega)^2 \quad (3)$$

intensity,  $\theta_{2\omega}$  is the angle from the surface normal at which the SHG signal occurs, and the vectors  $\mathbf{e}(\omega)$  and  $\mathbf{e}(2\omega)$  describe the polarization state and Fresnel factors for the fundamental and second harmonic light fields at the interface. This equation has been derived previously,<sup>30,77</sup> and can be used to describe a variety of experimental geometries including the case of total internal reflection. The components of  $\mathbf{e}(\omega)$  and  $\mathbf{e}(2\omega)$  for the external reflection geometry employed in the experiments in this paper have been presented in detail elsewhere.<sup>24</sup> Using eq 3, the elements of  $\chi_s^{(2)}$  can be extracted from the polarization dependence of the SHG. This polarization dependence is obtained by measuring the p-polarized (parallel to the plane of incidence) and s-polarized (perpendicular to the plane of incidence) second harmonic light intensities,  $I_p(2\omega)$  and  $I_s(2\omega)$ , respectively, as a function of the input polarization.<sup>72</sup> Once the relative magnitudes of  $\chi_{ZZZ}$ ,  $\chi_{ZXX}$ , and  $\chi_{XXZ}$  are obtained, they can then be used to describe the average molecular orientation at the interface via eq 2. For example, for a monolayer of molecules with only one dominant tensor element,  $\beta_{ZZZ}$ , an orientation parameter  $D$  can be obtained:<sup>78</sup>

$$D = \frac{\langle \cos^3 \theta \rangle}{\langle \cos \theta \rangle} = \frac{\chi_{ZZZ}}{\chi_{ZZZ} + 2\chi_{XXZ}} \quad (4)$$

Eq 4 has been used frequently to obtain molecular orientation information for adsorbed molecules at condensed phase interfaces.<sup>29</sup> Often an average orientation angle  $\langle \theta \rangle$  is reported, where it is assumed that the ensemble averages in eq 4 reduce to  $\cos^3 \langle \theta \rangle$  and  $\cos \langle \theta \rangle$ .<sup>78,72</sup> Different equations are required if other  $\beta$  elements are present in the molecule, and have been derived elsewhere.<sup>72</sup>

If the orientation parameter  $D$  does not change as a function of surface coverage, it can be seen from eqs 2 and 3 that the SHG intensity will be proportional to the square of the surface concentration of surfactant molecules. The square root of the surface SHG signal has been frequently employed as a relative measure of adsorbate surface coverage at various surfaces.<sup>29</sup> In this paper, the square root of the surface SHG signal is used to monitor the relative surface coverage of *trans*-DBA as a function of aqueous pH and concentration in DCE, as well as during photochemical conversion of the adsorbed monolayer to *cis*-DBA.

## Experimental Considerations

The surfactant molecule 4-[[[dodecyloxy]benz-4-yl]azo]benzoic acid (DBA) was synthesized and characterized as described previously.<sup>24</sup> DBA is soluble in DCE but not in water, and the organic phase in all of the SHG experiments was 10–25 mL of a 20  $\mu$ M DBA solution in DCE (Mallinckrodt SpectrAR grade). The aqueous phase consisted of 10–25 mL of a 10 mM  $\text{Na}_2\text{HPO}_4$  buffer solution adjusted to a pH of 9.0. In the experiments described in section C of the Results and Discussion, 50 mM NaCl and 1 mM tetrabutylammonium tetraphenylborate (TBATPB) were added to the aqueous and organic phases, respectively. Prior to the SHG experiments, the two phases were preequilibrated by thorough mixing in a separatory funnel, and were then allowed to equilibrate and re-separate for at least 1 h before measurements were taken. All experiments were performed at room temperature.

The SHG cell for the liquid/liquid experiments consisted of a 10  $\times$  40  $\times$  45 mm rectangular UV quartz cuvette which created a liquid/liquid interface with a total area of 4 cm<sup>2</sup> (Figure

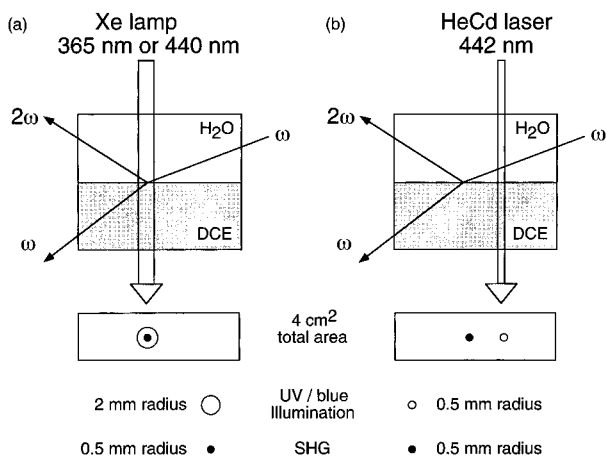


**Figure 2.** Schematic diagrams of the photoisomerization/SHG experiments. Surface SHG from a fundamental laser beam at  $\omega$  (730 nm) is collected in reflection through the aqueous phase. The fundamental light is incident on the water/dichloroethane interface at  $68^\circ$ , and surface SHG is detected at  $58^\circ$  from the normal to the interface. (a) Light from a Xe lamp at 365 or 440 nm is directed onto the interface concentric with the SHG laser spot. (b) A HeCd laser beam at 442 nm is focused onto the interface either concentric with the SHG laser spot or separated from it by up to 8 mm.

2). The experimental apparatus used for the SHG measurements has been described previously.<sup>24</sup> The SHG experiments employed an external reflection geometry, with the 730 nm fundamental laser beam at an angle of incidence of  $68^\circ$  on the interface, and the reflected second harmonic beam at 365 nm occurring at an angle of  $58^\circ$ . The SHG probe laser spot was approximately  $0.75 \text{ mm}^2$ , and power densities ranged from 30 to  $80 \text{ MW cm}^{-2}$ . In this range of laser power density, no SHG was observed from the water/DCE interface in the absence of DBA.

The photoisomerization experiments were performed by the addition of either a Xe lamp or HeCd laser as shown in Figure 2. The output of the Xe lamp (ILC Technology) was first filtered through a copper sulfate solution to remove all wavelengths above 540 nm and below 330 nm, and then the desired illumination wavelength was selected using an interference filter (Ealing) with a band pass of  $\pm 5 \text{ nm}$ . This light was then focused to a  $13 \text{ mm}^2$  spot concentric with the 730 nm SHG laser spot on the surface. The total intensity of the illumination from the Xe lamp onto the surface was 3 mW at 365 nm and 1 mW at 440 nm, resulting in power densities in the illumination spot of  $0.024$  and  $0.008 \text{ W cm}^{-2}$ , respectively. In a second set of experiments, the Xe lamp was replaced with a HeCd laser (Omnichrome). The HeCd laser line at 442 nm was selected with an interference filter, and was then focused onto the liquid/liquid interface in a spot the same size as the SHG laser spot ( $0.75 \text{ mm}^2$ ). This spot was directed onto the sample either concentric with the SHG laser spot or separated from it by up to 8 mm. The intensity of the HeCd beam was controlled with colored glass neutral density filters, and the power density on the surface was varied from  $0.02$  to  $0.8 \text{ W cm}^{-2}$ .

## Results and Discussion

**A. DBA Photochemistry in Solution.** The UV-vis spectrum of *trans*-DBA dissolved in DCE at a concentration of  $25 \mu\text{M}$  is shown in Figure 3 (the solid line). An absorption band is observed at 365 nm ( $\epsilon = 22\,500 \text{ L cm}^{-1} \text{ mol}^{-1}$ ) that is attributed to the  $\pi \rightarrow \pi^*$  charge transfer band for this molecule.<sup>39</sup> When the solution is illuminated with UV light at 365 nm, the *trans*-DBA molecules are converted to the *cis* isomer, and the 365 nm band decreases sharply in intensity. Two new bands

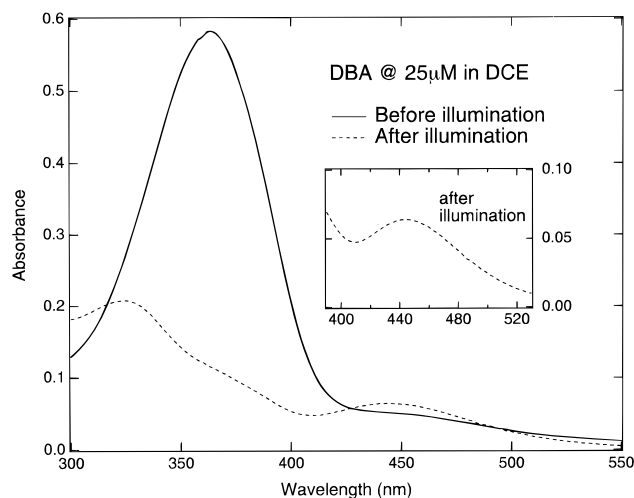


**Figure 3.** UV-vis spectrum of  $25 \mu\text{M}$  DBA in DCE before (solid line) and after (dashed line) illumination with 365 nm light. The spectrum before illumination corresponds to *trans*-DBA which exhibits a large absorption at 365 nm. As *trans*-DBA is converted to *cis*-DBA by 365 nm illumination, this band diminishes and new absorbances at 330 and 440 nm (inset) appear.

due to the *cis* isomer of DBA appear at 330 and 440 nm (see Figure 3). The band at 330 nm band is also the  $\pi \rightarrow \pi^*$  charge transfer band, shifted in energy for the new geometric and electronic structure of the isomer.<sup>38</sup> The band at 440 nm is attributed to an  $n \rightarrow \pi^*$  transition in the *cis*-DBA isomer. Upon illumination with light at 440 nm, the *cis*-DBA is converted back to the *trans* isomer and the UV-vis spectrum returns to the solid line in Figure 3. As the spectra of the *cis*- and *trans*-DBA overlap, illumination at a wavelength between the absorbance maxima at 365 and 440 nm results in the creation of a photostationary state composed of a mixture of *trans*- and *cis*-DBA. A photostationary state is established when a given wavelength of light stimulates both the forward and backward reactions of a photochemical equilibrium. The composition of the photostationary state depends upon the number of photons absorbed at that wavelength by both *trans*- and *cis*-DBA, and the quantum yields for the forward and back reactions. The quantum yields for photoisomerization in either direction are almost always greater when illuminated at the  $n \rightarrow \pi^*$  transition;<sup>39,38</sup> however, the  $n \rightarrow \pi^*$  transition in the *trans* isomer of azobenzenes is symmetry-forbidden and therefore very weak. Thus, the  $\pi \rightarrow \pi^*$  transition at 365 nm is almost always utilized for the *trans* to *cis* isomerization. The creation of photostationary states for monolayers of azobenzene derivatives at the air/water interface has been examined in detail by Maack *et al.*<sup>62,63</sup>

Since *cis*-azobenzenes are typically 50 kJ/mol higher in energy than their *trans* isomers,<sup>39</sup> *cis*-DBA is expected to slowly convert back to *trans*-DBA in the absence of further illumination. This thermal isomerization has a kinetic barrier of approximately 100 kJ/mol in most solvents, although the thermal isomerization rate of a substituted azobenzene depends strongly on which chemical groups are used to decorate the azobenzene and in which positions they are placed.<sup>38</sup> Figure 4 shows the thermal reconversion of *cis*-DBA back to the *trans* isomer in DCE. This solution was first illuminated with 365 nm light for 1 h, and the absorbances at 365 and 440 nm were monitored as the *cis*-DBA thermally converted back to the more stable *trans* form. The data in the figure show that at least 80% of the *cis* isomer has converted to *trans*-DBA in 2 h, and the solution has almost completely recovered in 3 h. The solid lines are exponential fits with a decay time of 67 min (rate  $1.5 \times 10^{-3} \text{ min}^{-1}$ ). This value is in good agreement with other

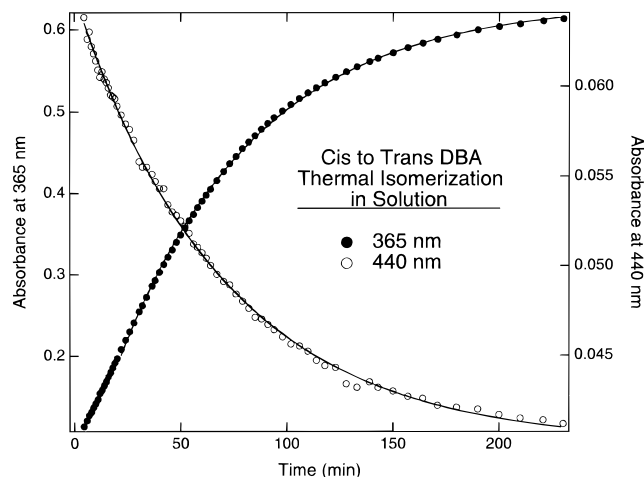


**Figure 4.** Thermal isomerization of *cis*- to *trans*-DBA in DCE solution. Absorbances at 365 nm (filled circles) and 440 nm (open circles) of DBA in DCE solution at room temperature are plotted as a function of time after the solution had been illuminated with 365 nm light. As *cis*-DBA is thermally converted back to the *trans* isomer, the absorbance at 365 nm (440 nm) increases (decreases). The solid lines are exponential fits with a decay time of 67 min.

thermal isomerization rates observed for substituted azobenzenes in solution.<sup>79,38,80</sup>

**B. Nonlinear Susceptibilities of *trans*- and *cis*-DBA.** As mentioned in the Background, the molecular nonlinear polarizability tensor  $\beta$  for molecules with a conjugated  $\pi$ -electron system is typically examined theoretically with a second-order perturbation theory calculation. This calculation employs a sum over all excited states, where the  $\pi$ -electron wave functions for these states are estimated by the semiempirical Pople–Pariser–Parr (PPP) wave functions. The various equations and details of this calculation have been presented elsewhere.<sup>72,24</sup> We have successfully used these semiempirical  $\beta$  calculations in a number of instances in order to predict the nonlinear optical behavior of various probe SHG molecules.<sup>24,81–83</sup>

Theoretical calculations of  $\beta_{zzz}$  for the *trans* and *cis* isomers of DBA are shown in Figure 5. In the case of the *trans* isomer, the transition dipole moment and the change in dipole moment are nearly colinear, resulting in a dominant  $\beta_{zzz}$  tensor element that is at least an order of magnitude larger than any other tensor element. A resonant enhancement in  $\beta_{zzz}$  is observed in the calculation at 675 nm for the DBA *trans* isomer. This enhancement corresponds to being in resonance at the second harmonic with the optical transition that is observed in DCE at 365 nm (the experimental resonance wavelengths are typically red-shifted from the PPP calculations due to solvation effects<sup>83</sup>). This corresponds to a fundamental laser frequency of 730 nm for surface SHG measurements. The absolute magnitude of this enhancement is 4 times that calculated for the smaller SHG probe molecule *p*-nitrophenol,<sup>83</sup> demonstrating that the azobenzene derivatives should in general serve as good surface SHG probe molecules.

Several changes occur in the molecular nonlinear polarizability tensor for DBA when converted from the *trans* to *cis* form. The first is that the transition dipole moment and the change in dipole moment are not colinear in the *cis*-DBA isomer, so that several  $\beta$  tensor elements of approximately equal magnitude are present, although only  $\beta_{zzz}$  is plotted in Figure 5. The second change in the molecular nonlinear optical response is that resonant enhancement at 730 nm is no longer present; instead, contributions from the transitions at 330 and 440 nm appear, corresponding to resonant enhancement of the SHG signal at 660 and 880 nm (note again that these

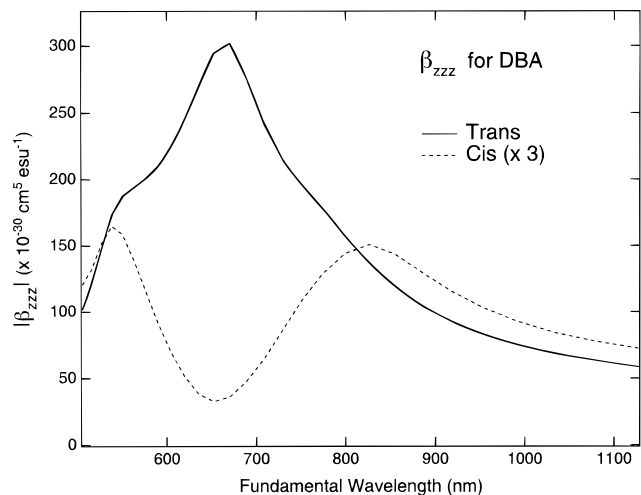


**Figure 5.** Calculation of the molecular nonlinear polarizability tensor element  $|\beta_{zzz}|$  as a function of fundamental laser wavelength for *trans* (solid line) and *cis* ( $\times 3$ , dashed line) DBA. The large enhancement shown at 675 nm for *trans*-DBA corresponds to the absorption in the UV–vis spectrum at 365 nm, resulting in an experimental fundamental laser wavelength of 730 nm. The experimental resonance wavelengths are red-shifted from the PPP calculations due to solvation effects. As the *trans*-DBA is converted to the *cis* isomer, the enhancement at 730 nm decreases and enhancements at 660 and 880 nm appear. This difference in enhancement in  $\beta$  at 730 nm suggests that SHG can be used to follow the photoisomerization of DBA at the water/DCE interface.

wavelengths are shifted in the essentially gas phase  $\beta$  calculation as compared to the wavelengths observed in DCE). However, both of these resonant enhancements (which are present in all  $\beta$  tensor elements) are smaller in magnitude than in the case of *trans*-DBA. This suggests that some resonant SHG signal from *cis*-DBA may be observable at either 660 or 880 nm, but surface SHG experiments performed at 730 nm should be much more sensitive to *trans*-DBA than to *cis*-DBA due to the strong difference in resonant enhancement at that wavelength. This fact will be used in this paper to follow the photoisomerization of a DBA monolayer at the water/DCE interface.

**C. DBA Adsorption and Acid–Base Chemistry at the Water/DCE Interface.** In a previous paper,<sup>24</sup> we examined the adsorption of *trans*-DBA to the water/DCE interface. Since DBA has a long organic tail and a hydrophilic head group, it should act as a surfactant and adsorb spontaneously from the organic phase to the liquid/liquid interface. However, surface SHG experiments showed that adsorption from micromolar DCE solutions only occurred when the pH of the aqueous solution was greater than 6.5, suggesting that the DBA carboxylate anion is the species adsorbed at the interface. The surface SHG at 730 nm observed from the water/DCE interface for a 20  $\mu\text{M}$  DBA organic phase is shown as a function of aqueous solution pH in Figure 6. A maximum amount of DBA was observed for an aqueous pH  $\geq 9$ ; from interfacial tension measurements,<sup>84</sup> an approximate maximum surface coverage of  $10^{14}$  molecules  $\text{cm}^{-2}$  was obtained.<sup>24</sup> A polarization analysis of the surface SHG signal resulted in an orientation parameter  $D$  of 0.77 ( $\theta = 29^\circ$ ); this orientation parameter did not change significantly as a function of pH.

The pH dependence of the DBA adsorption was also found to change with the DBA concentration in the DCE.<sup>24</sup> This dependence of the DBA adsorption on pH and solution concentration can be explained by a coupled equilibrium among neutral DBA in solution, neutral DBA at the interface, and the deprotonated DBA anion at the interface. If a Langmuir adsorption isotherm is assumed for the adsorption equilibrium,

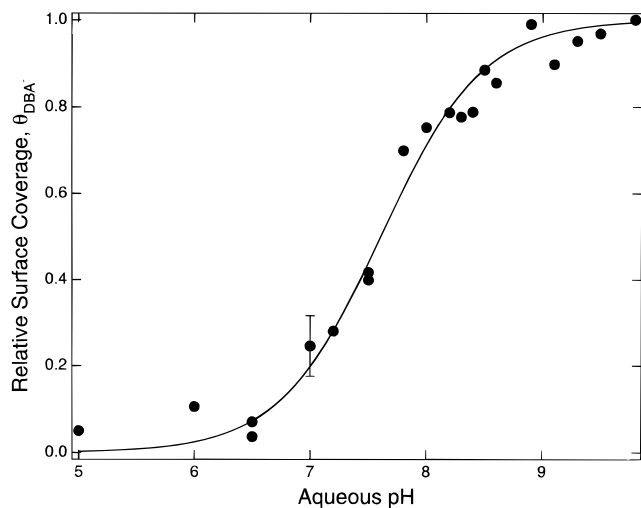


**Figure 6.** Relative surface coverage of DBA,  $\theta_{\text{DBA}^-}$ , (as determined from the square root of the surface SHG signal) at the water/DCE interface as a function of bulk aqueous pH. The aqueous phase contained 50 mM NaCl and 10 mM  $\text{Na}_2\text{HPO}_4$ , and the DCE phase consisted of 20  $\mu\text{M}$  DBA and 1 mM TBATPB. At a  $\text{pH} \leq 6.5$ , no adsorption of DBA is observed. As the aqueous pH is increased, the DBA coverage increases to a full monolayer ( $\theta_{\text{DBA}^-} = 1$ ) with an effective  $\text{p}K_a' = -\log(K_a^s K_{\text{ads}}^s [\text{DBA}]_d) = 7.6$ . This effective  $\text{p}K_a$  changed with the DBA concentration in the DCE. The solid line is a theoretical fit to eq 5 with  $K_{\text{ads}}^s K_a^s = 1.25 \times 10^{-3}$  (see the text for details). The data were taken from ref 24.

the surface coverage of the DBA anion,  $\theta_{\text{DBA}^-}$ , is found to follow eq 5, where  $[\text{H}^+]_s$  is the hydrogen ion activity at the

$$\theta_{\text{DBA}^-} = \left[ 1 + \frac{[\text{H}^+]_s}{K_{\text{ads}}^s K_a^s [\text{DBA}]_d} \right]^{-1} \quad (5)$$

interface,  $[\text{DBA}]_d$  is the activity of DBA in the DCE phase,  $K_{\text{ads}}^s$  is the Langmuir adsorption coefficient of the neutral surfactant to the interface, and  $K_a^s$  is the surface acid dissociation constant of DBA at the interface. A value of the product  $K_{\text{ads}}^s K_a^s$  of  $1.25 \times 10^{-3}$  was found to fit all of the pH and concentration dependence of the surface SHG signal (see ref 24 for a detailed discussion). The surface SHG measurements were also found to depend on the electrochemical potential applied across the interface via electrochemically induced changes in the interfacial hydrogen ion activity  $[\text{H}^+]_s$ ; this potential dependence was used to further characterize the nature of adsorption of the *trans*-DBA anion to the interface.<sup>24</sup>

#### D. DBA Photoisomerization at the Water/DCE Interface.

Since the *trans* and *cis* isomers of DBA exhibit different molecular nonlinear responses, the photoisomerization of *trans*-DBA anions adsorbed to the water/DCE interface can be observed with surface SHG measurements at a fundamental wavelength of 730 nm. In these experiments, the interface between a 20  $\mu\text{M}$  DBA dichloroethane phase and a basic (pH 9) aqueous phase is illuminated through the aqueous phase with a Xe lamp at either 365 or 440 nm (see Figure 2). The Xe light at the desired wavelength is focused on the interface, centered on the SHG spot but considerably larger (approximately a 2 mm vs 0.5 mm radius). Figure 7 illustrates the effect on the SHG signal from this illumination with UV light. The signal at the beginning of the experiment was due to the monolayer of *trans*-DBA at the interface. When the surface was exposed to the 365 nm light from the Xe lamp, the SHG signal dropped rapidly to approximately 23% of its original value. The magnitude of this drop was independent of laser power, and for the range of power densities reported in this paper, the time

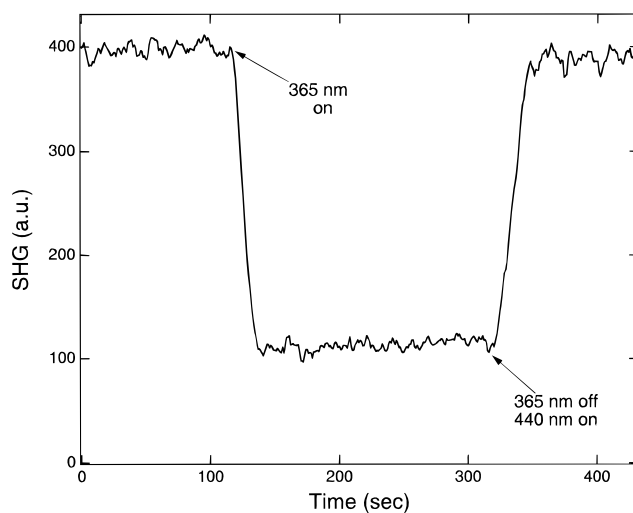


**Figure 7.** Surface SHG as a function of time during the illumination of the DBA monolayer with 365 and 440 nm light. The initial SHG is due to the monolayer of *trans*-DBA. When the 365 nm illumination starts, the signal drops rapidly (limited only by the time constant of the boxcar averager) to a new equilibrium level of SHG. The change in SHG is attributed to the conversion of *trans*-DBA to the *cis* isomer within the illumination spot. When 365 nm light is removed from the surface and 440 nm light is turned on, the SHG rapidly returns to its original level, restoring the DBA monolayer to the *trans* isomer.

scale of the drop in the SHG measurements was faster than the decay time of the boxcar averager used in these experiments (3 s). Upon illumination with 440 nm light from the Xe lamp, the surface SHG rapidly rose back to its original level. This loss and recovery of surface SHG signal was completely reversible, and could be repeated many times.

As mentioned in section B above, a decrease in SHG at 730 nm was expected upon the conversion of *trans*-DBA to *cis*-DBA at the water/DCE interface. A further consideration of the photoisomerization experiments reveals that SHG signal loss upon illumination with 365 nm could in principle arise from three different sources: (i) the conversion of adsorbed *trans*-DBA anions to the *cis* isomer, (ii) the desorption of molecules from the interface, or (iii) the reorientation of the *trans*-DBA at the interface. Slight changes in the polarization dependence of the SHG from the interface are observed after illumination at 365 nm; however, an analysis of the polarization dependence indicates that the tensor element ratio  $\chi_{zzz}:\chi_{zxz}:\chi_{xxz}$  changes from 6.2:1.0:1.0 to 6.6:0.9:1.0, which is far too small a change to account for the large decrease in the SHG signal.<sup>85</sup> In addition, independent interfacial tension measurements made before, during, and after illumination measured no change greater than  $0.1 \text{ dyn cm}^{-1}$  during the photoisomerization. These results indicate that it is unlikely that there is any photoinduced desorption of DBA from the interface. Also supporting this conclusion are the observations (i) that the signal very rapidly returns to its original level following illumination at 440 nm, and (ii) that the *cis*-DBA monolayer was very stable at the interface in the absence of illumination (see section E below). Thus, the only remaining possible source of signal loss during illumination is the conversion of the adsorbed DBA anions from the *trans* to the *cis* isomer, which has a weaker SHG response at 730 nm.

While the loss of signal upon illumination at 365 nm was significant (approximately 77%), it was not complete. The amount of residual SHG signal depends upon (i) the relative magnitudes of the *cis*- and *trans*-DBA molecular nonlinear polarizabilities at 730 nm and (ii) the steady state amounts of *trans*- and *cis*-DBA at the interface. Since we do not expect a

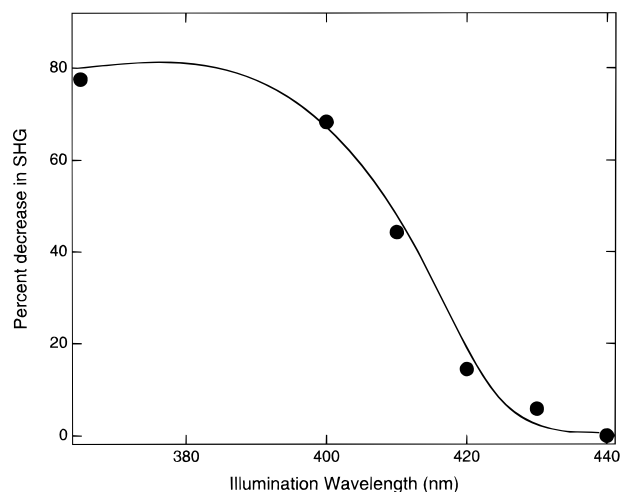


**Figure 8.** SHG signal drop at 365 nm during illumination as a function of the illumination wavelength. Maximum signal loss is achieved with an illumination wavelength of 365 nm (approximately 77%). No signal loss is observed with illumination at 440 nm (the absorption maximum for *cis*-DBA). At wavelengths 365 nm <  $\lambda$  < 440 nm, the SHG signal loss decreases monotonically, indicating that a photostationary state is being established at these wavelengths in the DBA monolayer at the water/DCE interface.

significant amount of resonant SHG from *cis*-DBA at 730 nm, and the polarization dependence of the surface SHG signal after illumination does not change significantly, we will assume that all of the surface SHG signal after illumination is due to residual *trans*-DBA. The continued presence of any *trans*-DBA anion at the surface during illumination at 365 nm is due to either (i) the creation of a photostationary state or (ii) the presence of a photoinactive surface population of the *trans* isomer. As shown in Figure 8, the amount of signal loss upon illumination varied with the wavelength of light used to illuminate the sample. At wavelengths close to 365 nm, the absorption maximum for *trans*-DBA, a maximum signal loss of close to 80% was achieved. At wavelengths between 365 and 440 nm (the peak absorption wavelength for *cis*-DBA), the magnitude of the signal loss decreased monotonically. At these intermediate wavelengths, a photostationary state where both isomers of DBA are constantly being formed and converted at the interface is definitely established. However, it should be noted that the illumination wavelength dependence of the surface SHG signal is not sufficient to determine whether *all* of the residual SHG signal is due to the *trans*-DBA isomer at the interface; this is a limiting assumption that we will make for the sake of concreteness in this paper. The portion of the *trans*-DBA that does photoisomerize will be called the “active *trans*” DBA for the rest of this paper, and a loss of 77% of the SHG signal using 730 nm fundamental light will be defined as 100% conversion of the active *trans*-DBA at the interface. It should also be noted that the same maximum amount of SHG signal loss (77%) could be achieved with either an interference filter passing only 365  $\pm$  5 nm or a colored glass filter passing 330–380 nm. Therefore, only excitation via the 440 nm transition of the *cis*-DBA results in reconversion to the *trans* isomer, and the 330 nm transition does not participate in the photoisomerization process.

The photoisomerization of azobenzenes has been studied at many different surfaces, but a complete conversion of the *trans*-DBA monolayer to the *cis* form is rarely observed. This incomplete conversion is usually attributed to low quantum yields in the photoisomerization process (resulting in a photostationary state) or steric hindrances in the isomerization process resulting from the molecular packing in a monolayer or film.

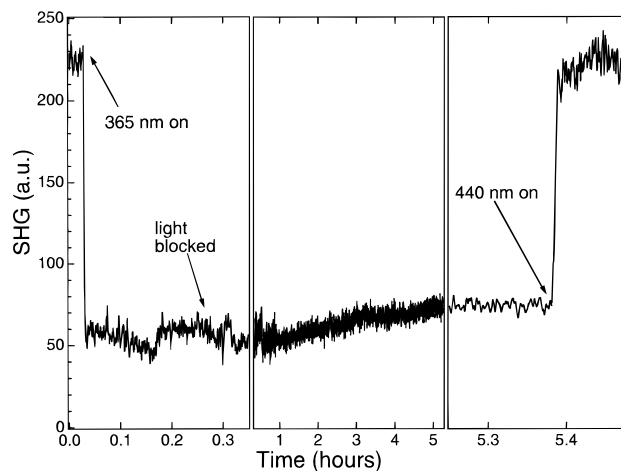


**Figure 9.** SHG from a DBA monolayer that has been completely converted to a maximum surface coverage of *cis*-DBA as a function of time. The sample is illuminated with 365 nm light for approximately 15 min, at which time all illumination except the SHG fundamental probe beam is removed. There is minimal recovery of the SHG over a period of > 5 h, indicating that *trans*-DBA is not returning to the surface. This demonstrates that the *cis* isomer of DBA is very stable at the water/DCE interface, and that the DBA monolayer is not exchanging molecules with the bulk DCE phase (see the text for details). After 5 h, the sample is exposed to 440 nm light, and full recovery of the SHG signal level and thus the *trans*-DBA monolayer is observed.

Since the SHG signal is proportional to the square of the surface coverage, if it is assumed that all the remaining SHG signal (23%) is due to residual *trans*-DBA, then approximately only half of the monolayer has been converted to *cis*-DBA. This number appears to be unusually low to attribute to only steric effects since other researchers have obtained conversion efficiencies of up to 90% with higher packing densities at the air/water interface.<sup>62,63</sup> It is possible, however, that the quantum yield of the reaction may be low at the water/DCE interface, resulting in an apparently “inactive” population of *trans*-DBA at the interface. The quantum yields are highly dependent on the temperature and medium, and relatively low quantum yields have been observed previously for similarly substituted azobenzenes.<sup>39</sup>

By changing the wavelength of the surface SHG experiment, we were able to verify that *cis*-DBA isomer was present at the interface. At a fundamental wavelength of 640 nm, the resonant contributions from the 330 nm transition in the *cis*-DBA are expected to be enhanced, and the loss of surface SHG signal upon illumination at 365 nm was observed to be only 50%, whereas the signal loss with a fundamental wavelength of 730 nm is 77% (data not shown). It can therefore be concluded that at least some contribution to the remaining SHG signal in this 640 nm experiment is from the *cis*-DBA anion at the water/DCE interface.

**E. Stability of the *cis*-DBA Anion at the Water/DCE Interface.** The previous section considered the photoisomerization of the *trans*-DBA anion to the *cis* isomer at the water/DCE interface during constant illumination at 365 nm. In fact, the *cis*-DBA created at this liquid/liquid interface was stable in the absence of UV light. If the surface was illuminated for over 450 s, all of the active *trans*-DBA over the entire interface was converted to the *cis*-DBA isomer. The time scale and transients observed during the surface conversion are examined in more detail in section F below. In Figure 9, the SHG signal from the surface is recorded for a 5 h period after an initial illumination at 365 nm for 15 min. During this time period, only a small amount of the *cis*-DBA is thermally converted back

to the *trans* form. Moreover, illumination with 440 nm light after 5 h resulted in a complete recovery of the original SHG signal.

The high stability demonstrated by the *cis*-DBA anions at the water/DCE interface is evidence that the adsorbed monolayer does not exchange DBA molecules with the bulk DCE solution. In section A, a thermal isomerization rate of  $(67 \text{ min})^{-1}$  was observed for DBA in DCE solution. If the monolayer were exchanging DBA molecules with the bulk organic phase, then the SHG would have returned to its original level on that time scale. We can therefore conclude that the monolayer of DBA anions at the liquid/liquid interface does not exchange molecules with the bulk organic phase at this high aqueous pH. Once created at the interface, the anionic DBA molecule cannot return to the organic phase without reprotonation, which is highly unlikely at an aqueous pH of 9. In addition, UV-vis measurements of the aqueous phase verify that no forms of DBA are photochemically transferred across the interface.

In comparison with azobenzene derivatives in other thin film systems, the *cis*-DBA anions at the water/DCE interface are remarkably stable. A similar azobenzene molecule assembled at the  $\text{SnO}_2/\text{air}$  interface was studied by Liu *et al.*,<sup>46</sup> who observed that 30% of the *cis* isomer was thermally reconverted back to the *trans* isomer in only 50 min at room temperature. Even when azobenzenes are covalently bound to a polymer in a film,<sup>55</sup> complete recovery of the *trans* isomer is accomplished in 8 h. While molecules in self-assembled monolayer films in general have slower thermal isomerization rates than those in bulk solution, there must be some additional chemical reasons why the *cis*-DBA is so stable at the water/DCE interface. Fujishima and co-workers have observed that reduced hydrazo compounds at interfaces are thermally stable,<sup>42,86</sup> but it is unlikely that photoreduction or photooxidation is occurring at the water/DCE interface. Another possible stabilizing mechanism at the liquid/liquid interface is intermolecular hydrogen bonding of the azo nitrogens with either the water molecules at the interface or other adsorbed DBA molecules.

**F. Photochemical Conversion of DBA over the Entire Interface.** As mentioned in the previous section, the entire active *trans*-DBA monolayer was converted to the *cis* isomer in 450 s upon illumination at 365 nm, despite the fact that only a small portion (about 3%) of the total interface was illuminated. To examine this conversion process in more detail, a series of SHG experiments with a variable illumination time were performed. Figure 10 shows the SHG signal after Xe lamp illumination at 365 nm for 220 s. The SHG signal drops initially to 23% of the original SHG signal as the maximum conversion level is quickly achieved within the Xe illumination spot. After the Xe lamp illumination is blocked, the SHG signal first rises and then settles to a steady state value. This new equilibrium level is due to the incomplete conversion of the total active *trans*-DBA monolayer on the surface to the *cis*-DBA isomer, followed by the reequilibration of the surface after the 365 nm illumination is blocked. The initial rise in SHG observed upon blocking of the 365 nm illumination varied from experiment to experiment; however, the variation in initial rise did not affect the steady state SHG level attained subsequently. Upon illumination with light at 440 nm, the entire surface is reconverted back to *trans*-DBA.

The new equilibrium SHG signal level established after conversion of a portion of the surface varied with the length of the illumination time on the sample, and is displayed in Figure 11. From the square root of this SHG signal level, the remaining fraction of the active *trans* monolayer can be calculated. This fraction,  $\theta_{\text{trans}}$ , is plotted in Figure 12 as a function of the square

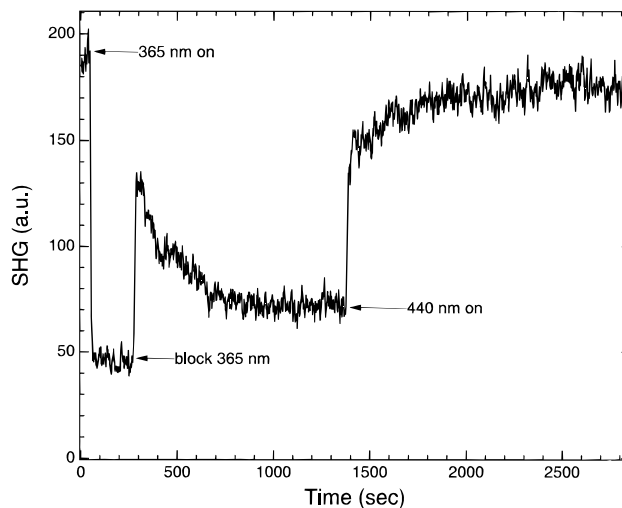


**Figure 10.** SHG as a function of time for a limited illumination time experiment. The sample is illuminated for 220 s with 365 nm light, at which time the illumination is blocked. During illumination, the SHG drops to a minimum as all active *trans*-DBA is converted to *cis* within the illumination spot. When the light is blocked, the SHG rises very quickly, and then settles to a new equilibrium level due to a redistribution of *cis*- and *trans*-DBA across the interface and in the laser spot. Full SHG recovery is subsequently observed upon illumination with 440 nm.

root of the illumination time. The conversion of the surface by illumination in a small spot can only occur if there is movement of the DBA molecules on the interface. If this is modeled as a case of surface diffusion, the remaining *trans* monolayer fraction should depend on the area of the interface,  $A$ , the radius of the illumination spot,  $B$ , and the illumination time,  $t_0$ , as shown in eq 6,<sup>87</sup> where  $D$  is the surface diffusion

$$\theta_{\text{trans}} = 1 - \frac{4B(\pi Dt_0)^{1/2}}{A} \quad (6)$$

constant for both the *trans* and *cis* isomers of DBA at the interface. The data in Figure 12 do follow eq 6, and analysis of these measurements produces a surface diffusion constant of  $0.025 \text{ cm}^2/\text{s}$ . This diffusion constant is about 4 orders of magnitude too large for physical diffusion on the surface,<sup>4,88,89</sup> or even in the bulk liquid.<sup>90</sup> Thus, other means of converting the surface must be considered.<sup>91</sup>

One possibility is that energy transfer from *trans*-DBA molecules within the 365 nm illumination spot to *trans*-DBA molecules on the surface could in principle lead to the rapid photochemical conversion of the entire monolayer from *trans*- to *cis*-DBA. During illumination, excited DBA molecules could be created via energy transfer outside of the illumination spot. These excited DBA molecules could then convert to the *cis* isomer. However, the SHG signal rises and reequilibrates to a new equilibrium level quickly after blocking the 365 nm light (see Figure 10). Since this rapid equilibration occurs in the absence of illumination, energy transfer must be ruled out as the primary reason for the anomalously fast surface conversion.

A second possible reason for the rapid photochemical conversion of the entire *trans*-DBA monolayer to the *cis* isomer is surface-tension-induced convection. Convection effects can arise via changes in the interfacial tension for different areas of the interface during the photoisomerization.<sup>92</sup> Changes in surface tension, due either to differences in *cis*- and *trans*-DBA surface coverage or local heating by the Xe lamp or HeCd laser, can lead to convective transport either directly or indirectly through the motion of the adjacent solution via the well-known Marangoni effect.<sup>92-94</sup> Surface-tension-induced convection and

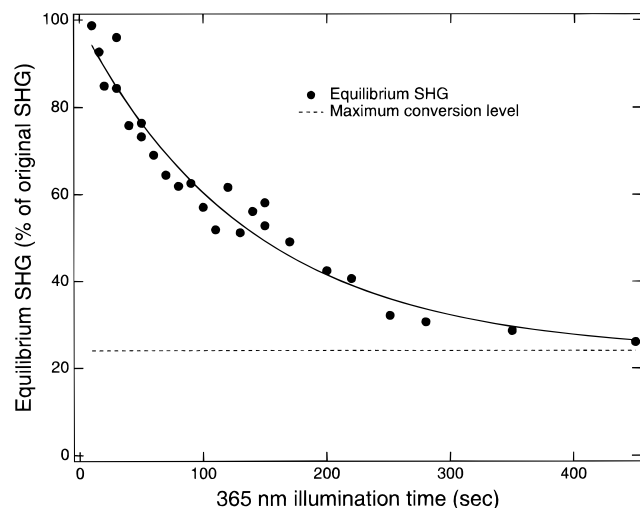


**Figure 11.** Amount of the original SHG signal observed upon surface reequilibration after a limited illumination time. The dashed line indicates the level of SHG that is achieved during illumination, when all of the active *trans*-DBA is converted to *cis*-DBA in the illumination spot. When the sample is illuminated for ca. 450 s, no recovery of the surface SHG is seen, indicating that the entire active interface has been converted to *cis*-DBA. At low illumination times, almost full recovery of *trans*-DBA SHG is observed. The solid line is an exponential fit with a decay time of 139 s.

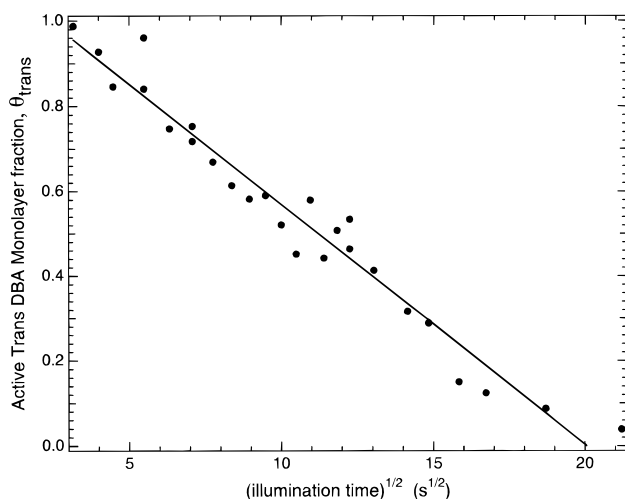


**Figure 12.** Remaining fraction of the active *trans*-DBA monolayer,  $\theta_{trans}$ , plotted versus the square root of the illumination time.  $\theta_{trans}$  is determined from the square root of the equilibrium SHG level in Figure 11. If the motion of DBA molecules at the water/DCE interface is modeled as surface diffusion, the slope of this plot yields a surface diffusion constant for DBA of  $0.025 \text{ cm}^2/\text{s}$  (see eq 6 in the text). This surface diffusion constant is 4 orders of magnitude larger than expected, implying that either surface convection or some other mechanism is responsible for the conversion of the entire interface.

large effective diffusion constants due to the Marangoni effect have been studied previously in monolayers at liquid/air interfaces.<sup>95,96</sup> Convection effects would also account for the rise in the SHG signal after the Xe lamp illumination is blocked; large fluctuations such as these would not occur if surface diffusion were the dominant transport mechanism.

As a final test that the entire monolayer of DBA was photochemically converted by a small illumination spot in less than 500 s, a set of SHG experiments were carried out where the illumination spot was well separated from the SHG probe laser spot. The Xe lamp was first used to convert the surface from *trans* to *cis* at 365 nm, and then a small spot from a HeCd laser at 442 nm was used to convert a part of the interface back to *trans*-DBA while recording the SHG signal from a different

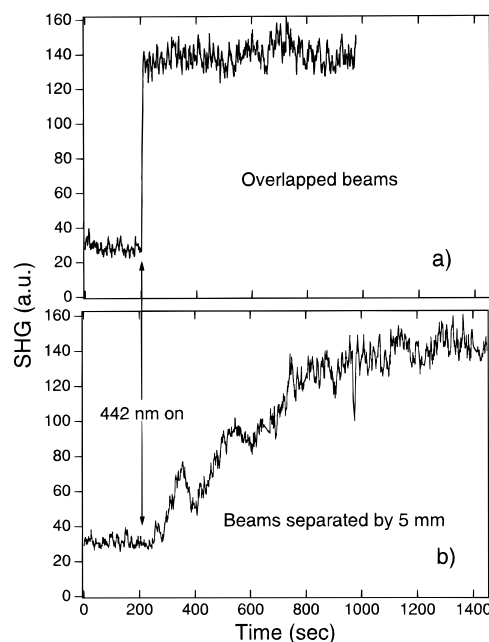


**Figure 13.** SHG as a function of time for *cis*-DBA monolayers being illuminated with 442 nm light from a HeCd laser where (a) the HeCd and SHG spots are overlapped and (b) the HeCd and SHG are separated by 5 mm. When the spots are overlapped, immediate return of the SHG is observed, similar to that seen in Figure 7. When the spots are separated, there is a delay between the start of the illumination and the onset of the SHG recovery. Full recovery of the SHG 5 mm away from the illumination spot is eventually achieved in approximately 1200 s, verifying that DBA molecules are moving across the entire water/DCE interface due to surface-tension-driven convection effects on a relatively fast time scale.

part of the interface (see Figure 2). Figure 13 shows the results of a typical two-spot experiment: when the HeCd and SHG were overlapped, an immediate recovery of the SHG in the laser spot was observed similar to that seen in Figure 7; if the beams were separated by 5 mm, then recovery of the SHG was still observed but on a longer time scale. This time scale is similar to the time scale observed in the Xe lamp experiments for total conversion of the surface to *cis*-DBA. In addition, anomalous waves in the surface SHG signal can be seen in the 5 mm data in Figure 13. The form of these anomalies varied from experiment to experiment, in a manner similar to that of the transient rise observed in Figure 10, and most likely was due to the interfacial-tension-induced convection currents that are responsible for equilibrating the entire surface.

A final experimental observation was that increasing the power of the HeCd illumination resulted in an increase in the rate of the return of the SHG signal level. Since the power density of the 442 nm light in all of the two-spot experiments was sufficient to rapidly convert all of laser spot from *cis*-DBA back to the *trans* isomer, any increase in the rate of conversion of the entire surface is due to increased laser heating effects, resulting in increased surface-tension-induced convection. This power dependence is further evidence that the DBA molecules were transported across the surface via surface convection induced by laser heating.

## Summary and Conclusions

In conclusion, we have demonstrated how the optical technique of resonant SHG can be used as a probe of photochemical reactions at the liquid/liquid interface. Due to changes in the molecular nonlinear polarizabilities between the *trans* and *cis* isomers, we were able to observe the *trans* to *cis*

photoisomerization process in a monolayer of an azobenzene derivative, DBA, adsorbed at the water/1,2-dichloroethane interface. The photoisomerization was reversible at this interface, and the *cis* form of the DBA molecule was found to be unusually stable. No appreciable thermal conversion of the *cis*-DBA to *trans*-DBA was observed over several hours. Complete conversion of the active surface from *trans*- to *cis*-DBA occurred on a very fast time scale that was attributed to surface mixing or surface-tension-driven convection effects.

**Acknowledgment.** The authors thank the National Science Foundation for support of this work and the Department of Defense for support through a National Defense Science and Engineering Graduate Fellowship (R.R.N.). The authors additionally thank Professor Johna Leddy for the derivation of the surface diffusion model and equations and Professor Robert Hamers for the use of the HeCd laser and Xe lamp.

## References and Notes

- Ahuja, R. C.; Mobius, D. *Thin Solid Films* **1994**, *243*, 547.
- Slotte, J. P.; Mattjus, P. *Biochim. Biophys. Acta* (Lipids and Lipid Metabolism section) **1995**, *1254*, 22.
- Prats, M.; Gabriel, B.; Teissie, J. *J. Am. Chem. Soc.* **1993**, *115*, 10153.
- Kovaleski, J. M.; Wirth, M. J. *J. Phys. Chem.* **1995**, *99*, 4091.
- Clark, D. C.; Mackie, A. R.; Wilde, P. J.; Wilson, D. R. *Faraday Discuss.* **1994**, *98*, 253.
- Watarai, H.; Saitoh, Y. *Chem. Lett.* **1995**, 283.
- Sassaman, J. L.; Wirth, M. J. *Colloids Surf., A* **1994**, *93*, 49–58.
- Piasecki, D. A.; Wirth, M. J. *J. Phys. Chem.* **1993**, *97*, 7700.
- Senda, M.; Kakiuchi, T.; Osakai, T. *Electrochim. Acta* **1991**, *36*, 253.
- (a) Koryta, J. *Electrochim. Acta* **1984**, *29*, 445. (b) Vanysek, P. *Electrochemistry on Liquid/Liquid Interfaces*; Springer-Verlag: New York, 1985.
- Schweighofer, K. J.; Benjamin, I. *J. Phys. Chem.* **1995**, *99*, 9974.
- Koryta, J. *Selective Electrode Rev.* **1991**, *13*, 133.
- Kakiuchi, T.; Kondo, T.; Senda, M. *Bull. Chem. Soc. Jpn.* **1990**, *63*, 3270.
- Beattie, P. D.; Delay, A.; Girault, H. H. *J. Electroanal. Chem.* **1995**, *380*, 167.
- Dvorak, O.; De Armond, M. K. *J. Electroanal. Chem.* **1991**, *317*, 299.
- Hanzlík, J.; Samec, Z.; Hovorka, J. *J. Electroanal. Chem.* **1987**, *216*, 303.
- Kakiuchi, T.; Noguchi, J.; Senda, M. *J. Electroanal. Chem.* **1992**, *327*, 63.
- Samec, Z.; Brown, A. R.; Yellowlees, L. J.; Girault, H. H.; Base, K. *J. Electroanal. Chem.* **1989**, *259*, 309.
- Yudi, L. M.; Santos, E.; Baruzzi, A. M.; Solís, V. M. *J. Electroanal. Chem.* **1994**, *379*, 151.
- Wandlowski, T.; Marecek, V.; Samec, Z. *J. Electroanal. Chem.* **1988**, *242*, 291.
- Nakanaga, T.; Takenaka, T. *J. Phys. Chem.* **1977**, *81*, 645.
- Higgins, D. A.; Naujok, R. R.; Corn, R. M. *Chem. Phys. Lett.* **1993**, *213*, 485.
- Higgins, D. A.; Corn, R. M. *J. Phys. Chem.* **1993**, *97*, 489.
- Naujok, R. R.; Higgins, D. A.; Hanken, D. G.; Corn, R. M. *J. Chem. Soc., Faraday Trans.* **1995**, *91*, 1411.
- Levinger, N. E.; Kung, K. Y.; Willard, D. M. *Abstracts of Papers*, 210th National Meeting of the American Chemical Society, Chicago, Fall 1995; American Chemical Society: Washington, DC, 1995; 6-COLL.
- Kott, K. L.; Higgins, D. A.; McMahon, R. J.; Corn, R. M. *J. Am. Chem. Soc.* **1993**, *115*, 5342.
- Shen, Y. R. *The Principles of Nonlinear Optics*; Wiley: New York, 1984.
- Eisenthal, K. B. *Annu. Rev. Phys. Chem.* **1992**, *43*, 627–661.
- Corn, R. M.; Higgins, D. A. *Chem. Rev.* **1994**, *94*, 107.
- Heinz, T. F. In *Nonlinear Surface Electromagnetic Phenomena*; Ponath, H. E., Stegeman, G. I., Eds.; North-Holland: Amsterdam, 1991; p 353.
- Shen, Y. R. *Annu. Rev. Phys. Chem.* **1989**, *40*, 327.
- Richmond, G. L. In *Electroanalytical Chemistry*; Bard, A. J., Ed.; Marcel Dekker, Inc.: New York, 1991; Vol. 17, p 87.
- Byers, J. D.; Hicks, J. M. *Chem. Phys. Lett.* **1994**, *231*, 216.
- Donaldson, D. J.; Guest, J. A.; Goh, M. C. *J. Phys. Chem.* **1995**, *99*, 9313.
- Grubb, S. G.; Kim, M. W.; Rasing, T.; Shen, Y. R. *Langmuir* **1988**, *4*, 452.
- Conboy, J. C.; Daschbach, J. L.; Richmond, G. L. *Appl. Phys. A* **1994**, *59*, 623.
- Tamburello Luca, A. A.; Hébert, P.; Brevet, P. F.; Girault, H. H. *J. Chem. Soc., Faraday Trans.* **1995**, *91*, 1763.
- Ross, D. L.; Blanc, J. In *Photochromism*; Brown, G. H., Ed.; Wiley-Interscience: Toronto, 1971; Vol. III, p 471.
- El'tsov, A. V. *Organic Photochromes*; Consultants Bureau: New York, 1990.
- Ikeda, T.; Tsutsumi, D. *Science* **1995**, *268*, 1873.
- Chaput, F.; Riehl, D.; Lévy, Y.; Boilot, J.-P. *Chem. Mater.* **1993**, *5*.
- Liu, Z.-F.; Hashimoto, K.; Fujishima, A. *Nature* **1990**, *347*, 658.
- Fujiwara, H.; Yonezawa, Y. *Nature* **1991**, *351*, 724.
- Ueno, A.; Yoshimura, H.; Osa, T. *J. Am. Chem. Soc.* **1979**, *101*, 2779.
- Willner, I.; Rubin, S.; Riklin, A. *J. Am. Chem. Soc.* **1991**, *113*, 3321.
- Liu, Z.-F. *J. Phys. Chem.* **1992**, *96*, 1875.
- Liu, Z.-F.; Hashimoto, K.; Fujishima, A. *Faraday Discuss.* **1992**, *94*, 221.
- Menzel, H.; Weichart, B.; Buchel, M.; Knoll, W. *Mol. Cryst. Liq. Cryst. Sci. Technol., Sect. A* **1994**, *246*, 397.
- Menzel, H. *Macromol. Chem. Phys.* **1994**, *195*, 3747.
- Yokoyama, S.; Kakimoto, M.; Imai, Y. *Langmuir* **1994**, *10*, 4594.
- Morigaki, K.; Liu, Z.-F.; Hashimoto, K.; Fujishima, A. *J. Phys. Chem.* **1995**, *99*, 14771.
- Wang, R.; Iyoda, T.; Hashimoto, K.; Fujishima, A. *J. Phys. Chem.* **1995**, *99*, 3352.
- Haitjema, H. J.; Vonmorgen, G. L.; Tan, Y. Y.; Challa, G. *Macromolecules* **1994**, *27*, 6201.
- Sekkat, Z.; Wood, J.; Knoll, W. *J. Phys. Chem.* **1995**, *99*, 17226.
- Barrett, C.; Natansohn, A.; Rochon, P. *Chem. Mater.* **1995**, *7*, 899.
- Naito, T.; Horie, K.; Mita, I. *Polymer* **1993**, *34*, 4140.
- Tanaka, M.; Sato, T.; Yonezawa, Y. *Langmuir* **1995**, *11*, 2834.
- Song, X.; Perlstein, J.; Whitten, D. G. *J. Am. Chem. Soc.* **1995**, *117*, 7816.
- Kawanishi, Y.; Suzuki, Y.; Sakuragi, M.; Kamezaki, H.; Ichimura, K. *J. Photochem. Photobiol., A* **1994**, *80*, 433.
- Sasaki, T.; Ikeda, T.; Ichimura, K. *Macromolecules* **1993**, *26*, 151.
- Ueda, M.; Kim, H.-B.; Ichimura, K. *Chem. Mater.* **1994**, *6*, 1771.
- (a) Maack, J.; Ahuja, R. C.; Tachibana, H. *J. Phys. Chem.* **1995**, *99*, 9210. (b) Ahuja, R. C.; Maack, J.; Tachibana, H. *J. Phys. Chem.* **1995**, *99*, 9221.
- Zhuang, X.; Lackritz, H. S.; Shen, Y. R. *Chem. Phys. Lett.* **1995**, *246*, 279.
- Guyot-Sionnest, P.; Chen, W.; Shen, Y. R. *Phys. Rev. B* **1986**, *33*, 8254.
- Goh, M. C.; Hicks, J. M.; Kemnitz, K.; Pinto, G. R.; Bhattacharyya, K.; Eisenthal, K. B.; Heinz, T. F. *J. Phys. Chem.* **1988**, *92*, 5074.
- Lantz, J. M.; Corn, R. M. *J. Phys. Chem.* **1994**, *98*, 4899.
- Lantz, J. M.; Corn, R. M. *J. Phys. Chem.* **1994**, *98*, 9387.
- Higgins, D. A. Ph.D. Thesis, University of Wisconsin—Madison, 1993.
- Li, D.; Marks, T. J.; Ratner, M. A. *Chem. Phys. Lett.* **1986**, *131*, 370.
- Li, D.; Ratner, M. A.; Marks, T. J. *J. Am. Chem. Soc.* **1988**, *110*, 1707.
- Albert, I. D. L.; Das, P. K.; Ramasesha, S. *Chem. Phys. Lett.* **1986**, *168*, 454.
- Corn, R. M.; Higgins, D. A. In *Characterization of Organic Thin Films*; Ulman, D. A., Ed.; Butterworth-Heinemann: Boston, 1995; pp 227–247.
- Nonlinear Optical Properties of Organic Molecules and Crystals*; Chemla, D. S., Zyss, J., Eds.; Academic Press, Inc.: Toronto, 1987.
- Dossen, G.; Drabe, K. E.; Wiersma, D. A.; Schoondorp, M. A.; Schouten, A. J.; Hulshof, J. B. E.; Feringa, B. L. *Langmuir* **1993**, *9*, 1974.
- Loucif-Saïbi, R.; Nakatani, K.; Delaire, J. A.; Dumont, M.; Sekkat, Z. *Chem. Mater.* **1993**, *5*, 229.
- Sekkat, Z.; Dumont, M. *Appl. Phys. B* **1992**, *54*, 486.
- Mizrahi, V.; Sipe, J. E. *J. Opt. Soc. Am.* **1988**, *B5*, 660.
- Heinz, T. F.; Tom, H. W. K.; Shen, Y. R. *Phys. Rev.* **1983**, *A28*, 1883.
- Strausz, O. P.; Lown, J. W.; Gunning, H. E. In *Decomposition and Isomerisation of Organic Compounds*; Bamford, C. H., Tipper, C. F. H., Eds.; Elsevier Publishing Co.: New York, 1972; Vol. 5, pp 566–603.
- Gegiou, D.; Muszkat, K. A.; Fischer, E. *J. Am. Chem. Soc.* **1968**, *90*, 3907.
- Campbell, D. J.; Higgins, D. A.; Corn, R. M. *J. Phys. Chem.* **1990**, *94*, 3681.
- Higgins, D. A.; Byerly, S. K.; Abrams, M. B.; Corn, R. M. *J. Phys. Chem.* **1991**, *95*, 6984.

(83) Higgins, D. A.; Abrams, M. B.; Byerly, S. B.; Corn, R. M. *Langmuir* **1992**, *8*, 1994.

(84) Bard, A. J.; Faulkner, L. R. *Electrochemical Methods: Fundamentals and Applications*; John Wiley and Sons: Toronto, 1980.

(85) This polarization analysis assumes that the dielectric constant for the *trans*- and *cis*-DBA are the same. It is conceivable, yet unlikely, that changes in the dielectric constants exactly cancel the changes in the susceptibility tensor elements to create no apparent change in the SHG polarization dependence.

(86) Liu, Z. F.; Loo, B. H.; Hashimoto, K.; Fujishima, A. *J. Electroanal. Chem.* **1991**, *297*, 133.

(87) Leddy, J. Private communication.

(88) Kim, S. Ph.D. Thesis, University of Wisconsin—Madison, 1992.

(89) Birdi, K. S. *Lipid and Biopolymer Monolayers at Liquid Interfaces*; Plenum Press: New York, 1989.

(90) Welty, J. R.; Wicks, C. E.; Wilson, R. E. *Fundamentals of Momentum, Heat, and Mass Transfer*; John Wiley & Sons: Toronto, 1969.

(91) Agrawal, M. L.; Neuman, R. D. *J. Colloid Interface Sci.* **1988**, *121*, 366.

(92) Levich, V. G.; Krylov, V. S. In *Annual Review of Fluid Mechanics*; Sears, W. R., Ed.; Annual Reviews, Inc.: Palo Alto, CA, 1969; Vol. 1, pp 293–316.

(93) Adamson, A. W. *Physical Chemistry of Surfaces*; John Wiley & Sons: Toronto, 1990.

(94) Sterling, C. V.; Scriven, L. E. *AIChE J.* **1959**, 514.

(95) Bois, A. G.; Ivanova, M. G.; Panaiotov, I. I. *Langmuir* **1987**, *3*, 215.

(96) Dimitrov, D. S.; Paniotov, I.; Richmond, P.; Ter-minassian-saraga, L. *J. Colloid Interface Sci.* **1978**, *65*, 483.

JP960558M